

Nanoscale

Accepted Manuscript



This is an *Accepted Manuscript*, which has been through the Royal Society of Chemistry peer review process and has been accepted for publication.

Accepted Manuscripts are published online shortly after acceptance, before technical editing, formatting and proof reading. Using this free service, authors can make their results available to the community, in citable form, before we publish the edited article. We will replace this *Accepted Manuscript* with the edited and formatted *Advance Article* as soon as it is available.

You can find more information about *Accepted Manuscripts* in the [Information for Authors](#).

Please note that technical editing may introduce minor changes to the text and/or graphics, which may alter content. The journal's standard [Terms & Conditions](#) and the [Ethical guidelines](#) still apply. In no event shall the Royal Society of Chemistry be held responsible for any errors or omissions in this *Accepted Manuscript* or any consequences arising from the use of any information it contains.

Synthesis, self-assembly, and immunological activity of α -galactose-functionalized dendron-lipid amphiphiles

John F. Trant,^a Namrata Jain,^a Delfina M. Mazzuca,^b James T. McIntosh,^a Bo Fan,^c S.M. Mansour Haeryfar,^b Sebastien Lecommandoux,^d and Elizabeth R. Gillies*^{a,c}

^a Department of Chemistry and Centre for Advanced Materials and Biomaterials Research, The University of Western Ontario, 1151 Richmond Street, London, Canada, N6A 5B7; E-mail: egillie@uwo.ca

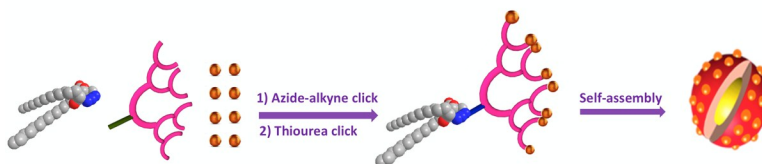
^b Department of Microbiology and Immunology, Department of Medicine, Centre for Human Immunology, Schulich School of Medicine and Dentistry, The University of Western Ontario, 1151 Richmond Street, London, Canada, N6A 5C1.

^c Department of Chemical and Biochemical Engineering, The University of Western Ontario, 1151 Richmond St., London, Canada, N6A 5B9.

^d Univ. Bordeaux; Bordeaux-INP ENSCBP; CNRS, Laboratoire de Chimie des Polymères Organique (LCPO), UMR 5629, 16 avenue Pey Berland, F-33600, Pessac, France.

Table of contents entry

A library of α -galactose-functionalized dendron-lipid hybrids were synthesized and the generation dependence of the self-assembly and bioactivity were studied.



Abstract

Nanoassemblies presenting multivalent displays of biologically active carbohydrates are of significant interest for a wide array of biomedical applications ranging from drug delivery to immunotherapy. In this study, glycodendron-lipid hybrids were developed as a new and tunable class of dendritic amphiphiles. A modular synthesis was used to prepare dendron-lipid hybrids comprising distearyl glycerol and 0 through 4th generation polyester dendrons with peripheral protected amines. Following deprotection of the amines, an isothiocyanate derivative of *C*-linked α -galactose (α -Gal) was conjugated to the dendron peripheries, affording amphiphiles with 1 to 16 α -Gal moieties. Self-assembly in water through a solvent exchange process resulted in vesicles for the 0 through 2nd generation systems and micelles for the 3rd and 4th generation systems. The critical aggregation concentrations decreased with increasing dendron generation, suggesting that the effects of increasing molar mass dominated over the effects of increasing the hydrophilic weight fraction. The binding of the assemblies to *Bandeirae simplicifolia* Lectin I (GSL 1), a protein with specificity for α -Gal was studied by quantifying the binding of fluorescently labeled assemblies to GSL 1-coated beads. It was found that binding was enhanced for amphiphiles containing higher generation dendrons. Despite their substantial structural

differences with the natural ligands for the CD1d receptor, the glycodendron-lipid hybrids were capable of stimulating invariant natural killer T (*i*NKT) cells, a class of innate-like T cells that recognize lipid and glycolipid antigens presented by CD1d and that are implicated in a wide range of diseases and conditions including but not limited to infectious diseases, diabetes and cancer.

Introduction

Carbohydrates play many important roles in biological systems including as structural components, energy sources, and as regulators of cellular communication, recognition, signaling and adhesion. These latter processes are normally mediated through either carbohydrate-carbohydrate or protein-carbohydrate interactions, and are critical aspects of many pathogeneses including viral and bacterial infection,^{1,2} immunological disorders,³ tumor formation⁴ and cancer metastasis.⁵ However, in all cases, these carbohydrate-based recognition events are non-covalent, and are generally quite weak.⁶ This reduces the effects of single, non-specific binding events, as multiple simultaneous interactions are often required to initiate biological processes.

Carbohydrate-mediated processes are often triggered by physical contact between two cells, or a virus and a cell, enabling multiple simultaneous carbohydrate-receptor interactions. For example, many influenza viruses interact with host cells through the binding of viral hemagglutinin proteins to sialic acid residues on the cell surface.⁷

The low affinity of carbohydrate interactions has limited the utility of carbohydrate-based therapeutic interventions in the past. One solution to this challenge has been to use irreversible inhibitors that covalently bind to the receptor and consequently inactivate it.⁸ However, covalent systems risk inactivating other enzymes when they are not highly selective.⁹ Another approach

takes inspiration from biology by using multivalent systems.¹⁰ Multivalent carbohydrates can exhibit enhanced binding through simultaneous interaction with multiple receptors, as well as through their high local concentration of ligand.¹¹

Several different systems have been explored for the development of multivalent carbohydrates,^{12, 13} including glycosylated synthetic peptides or polymers,^{14, 15} nanoparticles¹⁶ and self-assemblies including micelles,^{17, 18} liposomes,^{19, 20} and polymer vesicles.²¹⁻²³ The use of dendrons conjugated to or serving as the hydrophilic block in polymer assemblies can afford a high degree of multivalency due to the multiple peripheral groups on the dendron.²⁴⁻²⁷ In addition, the step-wise synthesis of dendrons affords well-defined products, allowing the number of peripheral groups to be carefully controlled. Carbohydrate-functionalized dendrons have been conjugated to the hydrophilic blocks of polymer vesicles,^{28, 29} and have also served as the hydrophilic blocks of amphiphiles where linear or dendritic hydrocarbons³⁰⁻³⁷ or polypeptides³⁸ have served as the hydrophobic blocks. Percec *et al.* reported that amphiphilic Janus glycodendrimers could self-assemble into a wide range of hard and soft assemblies including spherical and tubular vesicles, rod-like micelles, cubosomes, and solid lamellae depending on the chemical structures of their hydrophobic and carbohydrate-functionalized hydrophilic dendrons.³⁴ On the other hand, the conformational rigidity of the poly(γ -benzyl-L-glutamate) in the polypeptide-dendron system recently reported by our group resulted in susceptibility to macroscopic aggregation and only one of the investigated systems formed well-defined micellar assemblies in aqueous solution.³⁸

Because of the interest in developing carbohydrate-functionalized nanomaterials for biomedical applications such as targeted drug delivery, immunotherapy and medical diagnostic probes,^{13, 39, 40} the entire assembly would ideally be constructed from non-toxic and well-defined

components. In this context, naturally occurring glycerides are attractive as potential hydrophobic blocks. Although, dendron-lipid hybrids based on glycerides have been previously reported and explored for applications such as drug delivery,⁴¹⁻⁴⁴ to the best of our knowledge, there are no prior reports of glycodendron-lipid hybrids based on true glycerides. We report here the synthesis of a library of generation 0 through 4 (G0 – G4) glycodendron-lipid hybrids based on glycerides and exploit the amphiphilic character of the molecules for the preparation of generation-dependent assemblies while at the same time the potential of both the lipid and carbohydrate moieties to play roles in the bioactivities of the molecules. Both the amphiphiles and their assemblies are characterized and the abilities of these new systems to bind to lectins and to stimulate invariant natural killer T (*i*NKT) cells *in vitro* in a generation-dependent manner are described.

Results and discussion

Design of carbohydrate-dendron-lipid hybrids

The carbohydrate moiety selected for the functionalization of the lipid-dendron hybrids was α -galactose (α -Gal).³⁰ There are currently very few examples of multivalent assemblies presenting α -galactose.^{23, 38} Although terminal α -galactose moieties are found in other mammals, they are not normally found in humans. They are often a sign of pathogenesis and can result in immunostimulatory effects.^{45, 46} For example, KRN 7000 (Figure 1), first isolated from a Okinawan marine sponge,^{47, 48} has shown considerable activity against cancer as well as for a number of other potential immunotherapeutic applications.⁴⁹ This activity derives from the anchoring of the lipid domain in the groove of the CD1d receptor, an MHC type 1 protein found on antigen-presenting cells. The exposed α -galactoside antigen-ligand complex then activates

NKT cells that stimulate the downstream immune response. With a lipid-carbohydrate motif, the current class of carbohydrate-dendron-lipid hybrids shows some structural homology to the native ceramides such as KRN 7000. The unnatural *C*-glycoside anomeric linkage was designed to enhance the chemical and biochemical stability of the sugar, as the native *O*-linkage is highly susceptible to cleavage by enzymes and acidic pH.^{50, 51} The *C*-glycoside analogue of KRN 7000 was found to exhibit greater biological activity against melanoma than the native compound, and this has been ascribed to its enhanced stability in physiological conditions.⁵²

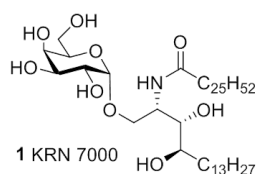


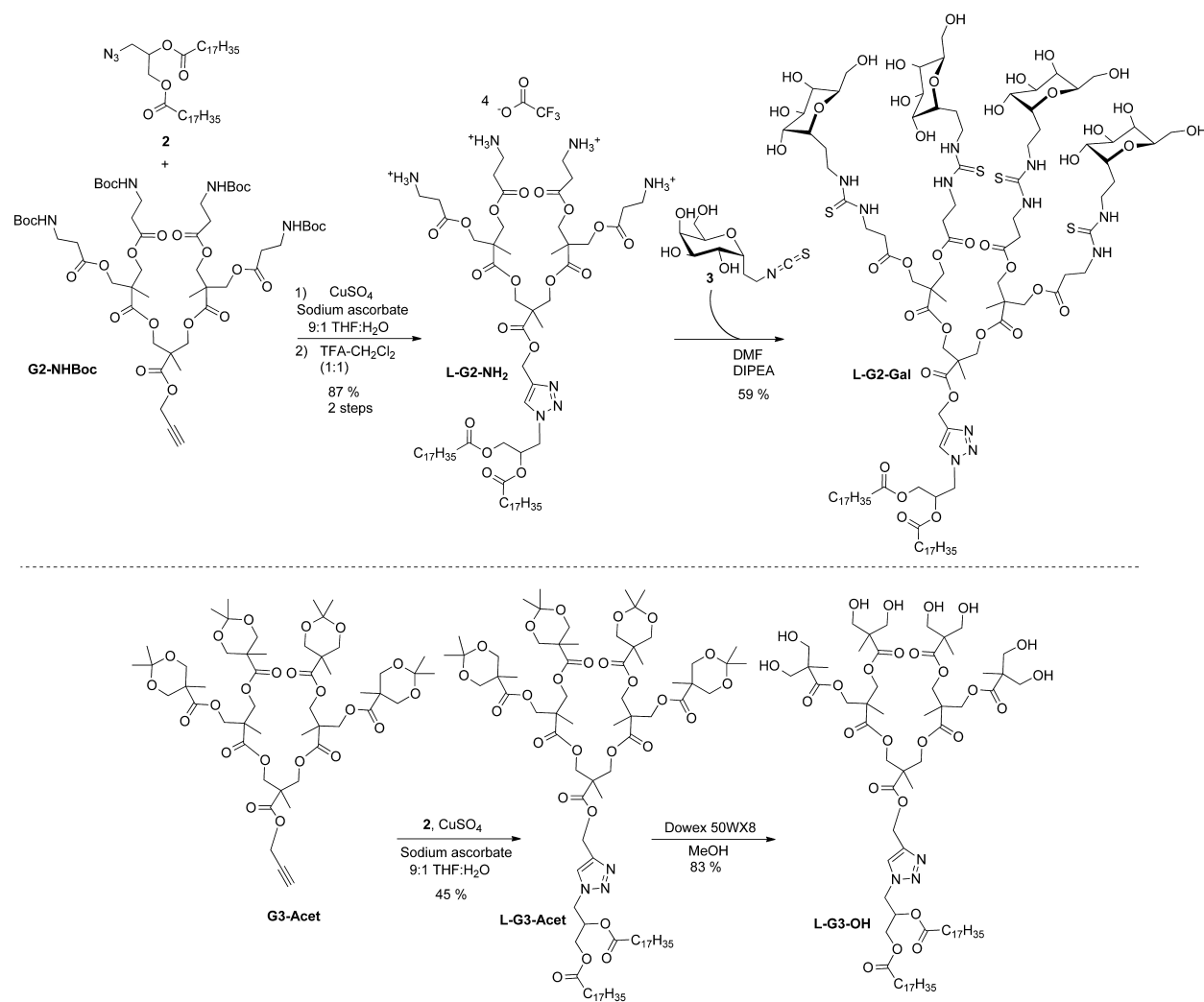
Figure 1. Structure of KRN 7000.

A 1,2-distearoylglycerol was selected as the lipid component of the amphiphiles as the two stearoyl chains contribute a similar total hydrophobic content to the combined C13 and C25 chains found in ceramide **1** (total of 34 vs 38 hydrophobic carbon atoms), while still retaining ease of synthesis with the two chains being identical. A dendron backbone based on 2,2-*bis*(hydroxymethyl)-propionic acid (bis-HMPA) was selected. This well-studied polyester scaffold has been shown to be non-toxic at relatively high concentrations *in vivo*,^{53, 54} can be readily prepared through a divergent strategy,^{55, 56} and is amenable to further functionalization.^{28, 57} The ester groups in this backbone also provide a good balance of chemical stability and degradability.⁵⁸ Zero through fourth generation (G0 - G4) dendrons were employed to provide 1 to 16 sites for functionalization with carbohydrates.

Synthesis of carbohydrate-dendron-lipid hybrids

A modular synthesis was employed, involving the conjugation of an azide-functionalized 1,2-distearoylglycerol to G0 – G4 polyester dendrons with focal point alkynes, followed by functionalization of the dendron's peripheral groups with α -galactose. Carbohydrate conjugation was reserved for the last step because the sugars impart amphiphilicity to the molecules making them more challenging to carry through multiple steps of synthesis.

The azido diglyceride **2** (Scheme 1) was prepared from racemic glycidol according to a published protocol for a similar compound (ESI).⁵⁹ *t*-Butyloxycarbonyl (Boc)-protected β -alanine functionalized polyester dendrons with focal point alkynes were also prepared as previously reported,³⁸ with the exception of the previously unreported G1 system, the procedure for which is provided in the ESI. As shown in Scheme 1 for a second generation dendron (**G2-NHBoc**), coupling to **2** was then performed using modified Sharpless-Fokin Cu-assisted azide-alkyne cycloaddition conditions^{60, 61} to provide **L-G2-NHBOC**. The resulting lipid-dendron hybrids were purified chromatographically and then the Boc protecting groups were removed using 1:1 trifluoroacetic acid (TFA):CH₂Cl₂ to afford the amine-functionalized dendron-lipid hybrid **L-G2-NH₂**. The isothiocyanate-activated α -C-galactoside **3** was prepared from galactose as previously reported.^{38, 61} It was coupled to the amine-functionalized dendron-lipid hybrid in *N,N*-dimethylformamide (DMF) in the presence of *N,N*-diisopropylethylamine (DIPEA) to afford the carbohydrate-dendron-lipid hybrid **L-G2-Gal**. The same methods were used to prepare G0 through G4 systems shown in Figure 2, except that for the G0 system, Boc-protected propargyl amine was used instead of a dendron. The G1 through G4 products were purified by dialysis in DMF followed by H₂O to remove excess carbohydrate and salts while the G0 system was purified by preparative thin layer chromatography.



Scheme 1. Representative synthesis of a α -Gal-functionalized lipid-dendron hybrid as well as a hydroxyl-functionalized control.

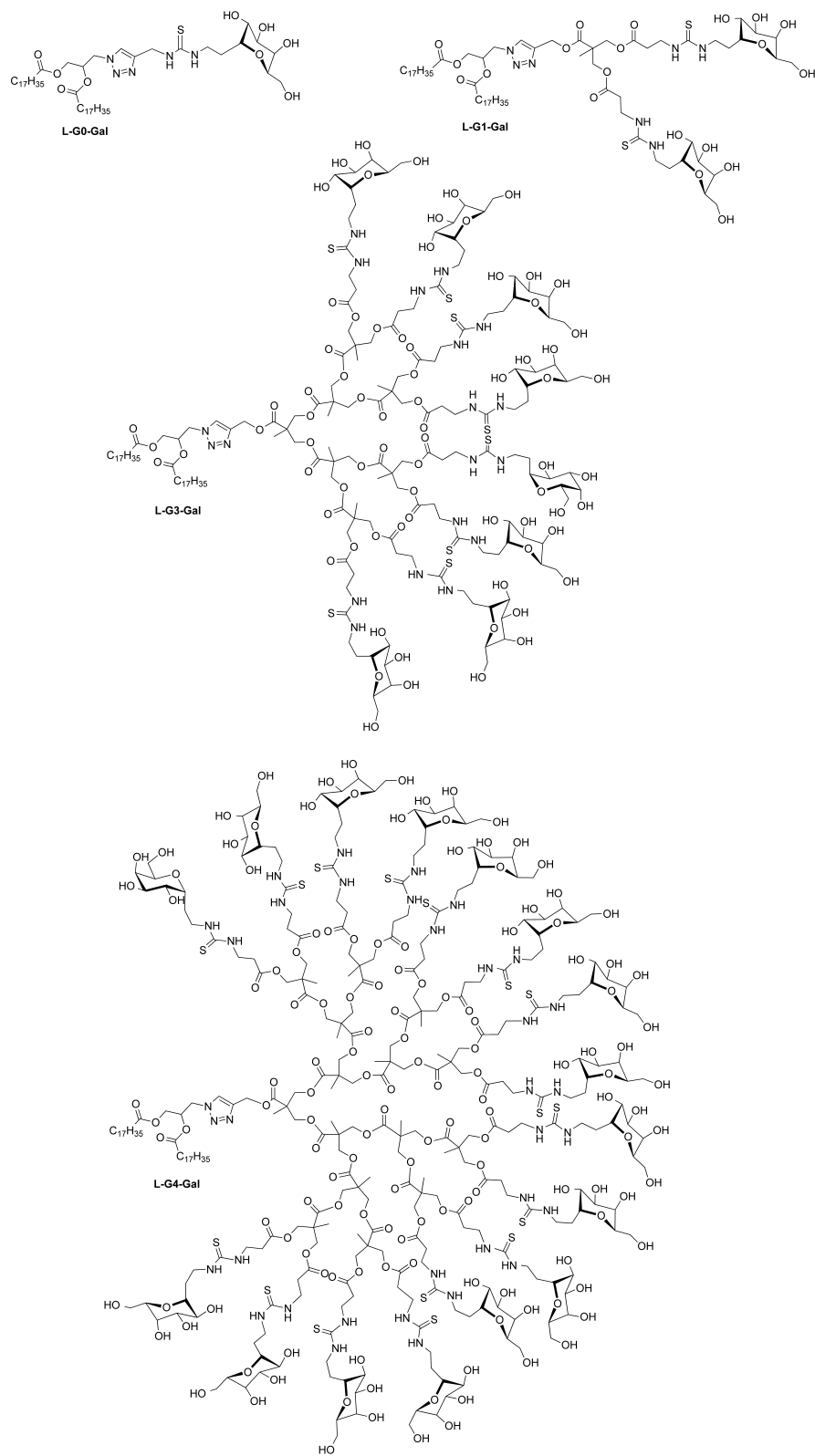


Figure 2. Chemical structures of the α -Gal-functionalized dendron-lipid hybrids.

Using an analogous strategy, a control G3 system with peripheral hydroxyls instead of carbohydrates was also prepared by coupling acetonide-protected G3 (**G3-Acet**)⁵⁵ with **2** to afford **L-G3-Acet** (Scheme 1). The acetonide groups were subsequently removed by treatment with acidic DowexTM 50WX8 resin in methanol to provide **L-G3-OH**. This product was purified chromatographically. All dendron-lipid hybrids were characterized by ¹H and ¹³C NMR spectroscopy. Based on the relative integrations of the ¹H NMR peaks corresponding to the isothiocyanate-functionalized versus unreacted β -alanine moieties at the dendron peripheries, the extent of functionalization ranged from ~80% for **L-G2-Gal** to more than 90% for all of the other α -Gal-functionalized hybrids. Peak assignments and details of this analysis are included with the corresponding spectra in the ESI. Mass spectrometry was also used to confirm the structural assignment of all final materials and intermediates except for **L-G3-Gal** and **L-G4-Gal**, where fragmentation processes dominated. Spectra and details of these analyses are also included in the ESI.

In addition, the glass transition temperatures (T_g) and melting points (T_m) were determined by differential scanning calorimetry (DSC). As shown in Table 1, upon increasing the generation of the α -Gal-functionalized dendron, the molecules transitioned from being crystalline or semicrystalline solids with the T_m ranging from 56 °C for the G0 system to 18 °C for the G3 system to an amorphous solid at G4. This suggests that higher dendron generations interfere with crystalline packing, resulting in smaller crystalline domains and thus lower T_m . In contrast, the T_g increased from -8 °C for the G3 system to 12 °C for the G4 system, indicating reduced segmental motion at higher generations. For comparison, the lipid derivative **2** is a crystalline solid with a T_m of 38 °C, while the previously reported galactose-functionalized polyester dendron (Propargyl-G3-Gal)³⁸ is an amorphous solid with a T_g of -8 °C. Thus, the crystalline

behavior of the lipid dominates at lower dendron generations while the amorphous properties of the dendron dominate at higher dendron generations.

Table 1. Overview of the dendron-lipid hybrids (ND = none detected).

Compound	Dendron generation (number of peripheral groups)	T _g	T _m
L-G0-Gal	0 (1)	ND	56 °C
L-G1-Gal	1 (2)	ND	53 °C
L-G2-Gal	2 (4)	ND	36 °C
L-G3-Gal	3 (8)	-7 °C	18 °C
L-G4-Gal	4 (16)	12 °C	ND
L-G3-OH	3 (8)	-14 °C	38 °C
Lipid derivative 2	-	ND	38 °C
Propargyl-G3-Gal ³⁸	3 (8)	-8 °C	ND

Self-assembly of carbohydrate-functionalized dendron-lipid hybrids

The hydrophilic mass fractions (f) of the carbohydrate-dendron-lipid hybrids were calculated as the molar mass of the hydrophilic fraction/(total molar mass). For the **Gal** series, the hydrophilic fraction was considered to be the mass of the carbohydrate residues alone, while for **L-G3-OH** it was considered to be only the mass of the hydroxyl groups, as the polyester dendrimer backbone is hydrophobic. As shown in Table 2, **L-G3-OH** had an f value of 0.09, while f ranged from 0.17 to 0.34 for the α -Gal-functionalized materials as the dendron generation increased from G0 to

G4. It was anticipated that as both the curvature and f increase with increasing generation, a transition from lamellar to micellar morphologies would be observed.

Table 2. Properties of assemblies formed by dendron-lipid amphiphiles as determined by DLS and TEM. ^aFrom the DLS intensity distribution.

Amphiphile	f	Peak diameter(s) ^a (DLS, nm)	Z-Average diameter (DLS, nm)	Dispersity (from DLS)	Morphology from TEM (organic solvent)
L-G0-Gal	0.17	310	290	0.08	Vesicles (THF)
L-G1-Gal	0.22	250	260	0.39	Vesicles (THF)
L-G2-Gal	0.28	190	190	0.36	Vesicles (DMSO)
L-G3-Gal	0.32	10, 220	15	0.57	Micelles, aggregates of micelles (DMSO)
L-G4-Gal	0.34	10, 170	60	0.16	Micelles, aggregates of micelles (DMSO)
L-G3-OH	0.090	145	120	0.19	Compound micelles (DMSO)

The self-assembly of the amphiphiles was investigated by a solvent exchange method. Due to the differing solubilities of the different generations, THF was selected as the organic solvent for the G0 and G1 systems, while DMSO was used for the G2 through G4 systems. The reported results correspond to the assemblies obtained by the addition of water to the organic solution of the amphiphile, although the addition of the organic solution to water gave similar results. The assemblies were characterized by dynamic light scattering (DLS) (Table 2 and ESI) and transmission electron microscopy (TEM) (Figure 3). **L-G0-Gal**, **L-G1-Gal**, and **L-G2-Gal** appeared to self-assemble into dendrimersomes with diameters ranging from ~200-300 nm (Figure 3a-c). The hydrodynamic diameters measured by DLS were in general agreement with the diameters observed by TEM (Table 2). In comparison with previously reported Janus glycodendrimers,^{31, 33, 34, 62} the current amphiphiles were able to tolerate a higher carbohydrate:alkyl chain ratio while still retaining the vesicular morphology. This may be attributed to the hydrophobic polyester backbone supporting the display of the carbohydrates in comparison to the shorter and/or more hydrophilic spacers previously reported. Based on their sizes and solid morphologies observed in TEM (Figure 3d and 3e), both **L-G3-Gal** and **L-G4-Gal** self-assembled to form mainly micelles. This change in morphology from vesicles to micelles can be attributed to the increased curvature and increased hydrophilic fraction of these higher generation systems. Based on DLS analysis, the micelle hydrodynamic diameters of both the G3 and G4 systems were approximately 10 nm, but some aggregates with diameters closer to 200 nm were also observed, which influenced the Z-average diameters of these assemblies. Aggregates of micelles could also be observed by TEM (Figures S80 and S81). The **L-G3-OH** amphiphile assembled to form solid particles that based on DLS and TEM data were likely compound micelles.

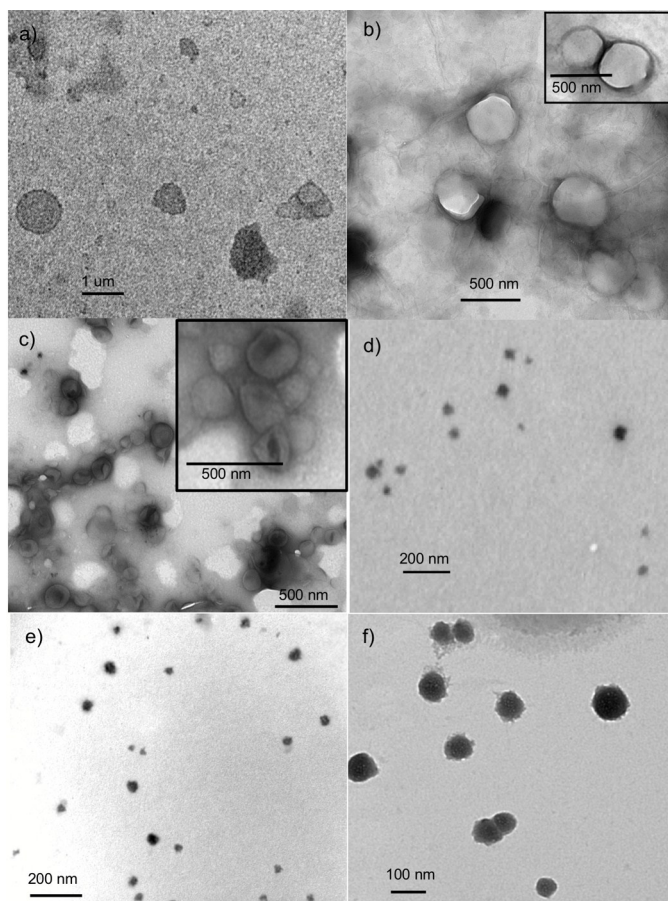


Figure 3. Representative TEM images of assemblies formed from a) **L-G0-Gal**; b) **L-G1-Gal**; c) **L-G2-Gal**; d) **L-G3-Gal**; e) **L-G4-Gal**; f) **L-G3-OH**.

The critical aggregation concentration (CAC) for each amphiphile was determined in 0.1 M, pH 7.4 phosphate buffer using pyrene as a fluorescent probe.^{63, 64} This method exploits the differences in the emission spectra of pyrene in environments with different polarizability to determine the presence or absence of hydrophobic domains. As shown in Table 3, the CACs ranged from 118 mg/L for **L-G0-Gal** to 20 mg/L for **L-G4-Gal**. Similar values were also obtained using a procedure based on DLS.⁶⁵ In terms of molarity-based concentrations, this corresponds to a nearly two orders of magnitude decrease in the CAC as the dendron generation was increased from G0 to G4. Initially, it was expected that the CAC would increase with

increasing f , and thus increasing dendron generation. For example, Suck and Lamm⁶⁶ predicted that for hydrophilic dendrons of varying generation conjugated to a hydrophobic chain of fixed length, the CAC should increase with increasing dendron generation, which is in agreement with previously reported experimental results.^{37, 67, 68} However, the opposite trend was observed for the current system. Instead, the increase in the molar mass (MM) associated with higher dendron generation seems to dominate. This may result from the hydrophobicity of the polyester backbone, as increasing the dendron generation results in not only an increase in f but also an increase in the molar mass of the hydrophobic block, a parameter that is also known to result in decreasing CAC.⁶⁹ As shown in Figure S88, interestingly $\log(\text{CAC})$ exhibits a linear dependence on $\log(\text{MM})$ for this series of compounds.

Table 3. CACs for the dendron-lipid hybrids as measured by the pyrene probe and DLS methods.

Compound	CAC (pyrene, mg/L)	CAC (pyrene, nM)	CAC (DLS) (mg/L)	MM (g/mol)
L-G0-Gal	118	120	100	954
L-G1-Gal	50	34	100	1462
L-G2-Gal	37	16	30	2334
L-G3-Gal	27	6.6	15	4079
L-G4-Gal	20	2.6	20	7568
L-G3-OH	6	3.8	10	1518

Lectin binding studies

With the small library of α -Gal-functionalized assemblies in hand, binding to the α -galactose specific lectin, *Griffonia simplicifolia* Lectin I (GSL 1) isolated from a woody climbing shrub in West Africa,⁷⁰ was evaluated. This lectin is highly sensitive to structural modifications such as 2-deoxydation or alkylation,⁷¹ and to any modification of the C-6 hydroxymethyl as a 30-fold lower binding to D-fucosyl glycosides demonstrates.⁷² It is ~100-fold more selective for α -galactose over β -galactose.⁷² To the best of our knowledge, its binding to C-linked α -Gal has not previously been investigated.

There are many methods to quantitatively or semi-quantitatively evaluate the binding between lectins and carbohydrates.⁷³⁻⁷⁵ In the current work, the binding of fluorescently labeled carbohydrate-dendron-lipid assemblies to lectin-functionalized agarose beads was selected as the approach to compare the different assemblies.⁷⁶ To perform this assay, the assemblies were prepared in the presence of Nile red, a stable fluorescent dye that partitions into the hydrophobic domains of assemblies.⁷⁷ Following dialysis against 0.1 M, pH 7.4 phosphate buffered saline (PBS) to remove unincorporated Nile red and residual organic solvent, the fluorescence of each assembly was measured in order to later normalize the data (Table S1). Next, the assemblies were added to suspensions of GSL 1-coated agarose beads. The concentration of dendron-lipid hybrid in these studies was 0.25 mg/mL, above the CAC for each system. After 3 hours of incubation at ambient temperature, the beads were subjected to either one or two thorough washing procedures. Fluorescence microscopy was then used to quantify the fluorescence of the beads, with high fluorescence (Figure 4a) indicating the binding of more assemblies to the beads than low fluorescence (Figure 4b). After correcting for autofluorescence, the dark pixel effect

arising from differing exposure times,⁷⁸ and normalizing the data with respect to the fluorescence intensities of the different assemblies, a quantitative comparison of the binding of the different systems to the beads was obtained.

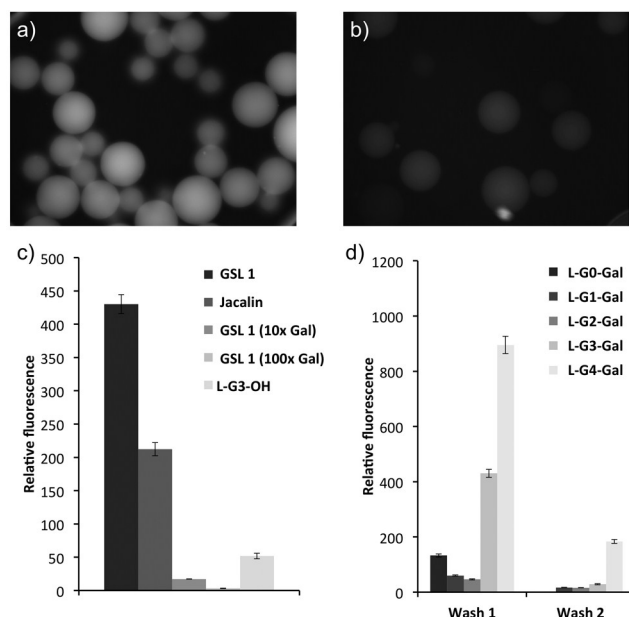


Figure 4. (a, b) Fluorescence microscopy images of GSL 1-coated agarose beads at 20x magnification. Image a) is of a highly fluorescent sample (**L-G3-Gal**) while image b) is of a weakly fluorescent sample (**L-G3-OH**) indicating poor binding to the bead. c) Normalized relative fluorescence of **L-G3-Gal** assemblies bound to GSL 1 or Jacalin-coated agarose beads in the absence or in the presence of excess free galactose; **L-G3-OH** assemblies bound to the beads are also included here for comparison. d) Relative fluorescence of GSL 1-coated beads incubated with varying generations of α -Gal-functionalized dendron-lipid hybrids and then subjected to one or two thorough washing procedures. Error bars represent the standard error on the mean of the measurements.

Experiments were also performed to ensure that the observed binding was specific. Despite their lack of carbohydrates, the **L-G3-OH** assemblies have many hydroxyl groups on their

surfaces and their binding to GSL 1-coated beads was evaluated. In addition, the binding of assemblies of **L-G3-Gal** to GSL 1-coated beads was evaluated in the presence of a 10-fold and 100-fold excess of free galactose. Furthermore, the binding of **L-G3-Gal** assemblies with Jacalin-coated agarose beads with the same lectin loading was evaluated. Jacalin is a plant-based lectin isolated from jackfruit,⁷⁹ that binds preferentially to β -galactosyl and β -2-*N*-acetyl-galactosyl residues, although it does show moderate binding to α -Gal moieties.⁸⁰

As shown in Figure 4c, **L-G3-Gal** exhibited ~2-fold higher binding to the GSL 1-coated beads than to the Jacalin-coated beads (surface lectin concentration for the two beads is identical), suggesting specificity for the lectin that binds α -Gal more strongly. In addition, the presence of 10-fold and 100-fold excess free galactose suppressed the binding of **L-G3-Gal** to GSL 1-coated beads 25-fold and 80-fold respectively. This dose-responsive competitive inhibition suggests that the **L-G3-Gal** assemblies bind specifically to the carbohydrate-binding site on GSL 1 rather than nonspecifically to the protein or bead itself. The **L-G3-OH** assemblies have significantly lower affinity for the GSL 1-coated beads than for the α -Gal system, again suggesting quite specific binding involving the carbohydrate moieties. Overall, this series of experiments demonstrated that *C*-linked α -Gal could still bind to GSL 1, and that it could do so in a specific manner even when conjugated to the periphery of a dendron and presented at the surfaces of nanoassemblies. This is despite the dense topography of the surface which has been suggested to significantly decrease lectin affinity due to steric crowding compared to a more freely displayed carbohydrate.³²

A comparison of the binding of the assemblies prepared from dendron-lipid hybrids of different generations after either one or two thorough washing procedures is shown in Figure 4d. The goal of the second wash protocol was to remove the more weakly bound and less stable

assemblies, thereby providing some additional information regarding the potential of the different systems. After the first wash, **L-G4-Gal** exhibited ~2-fold higher binding to GSL 1-coated beads than **L-G3-Gal**, and ~7-fold higher binding than **L-G0-Gal**. **L-G1-Gal** and **L-G2-Gal** were similar to one another and exhibited the lowest binding, which was ~18-fold lower than the best binder **L-G4-Gal**. To explain this rather parabolic trend in the binding with increasing generation, we suggest that the **L-G0-Gal** system exhibited moderate binding resulting from the presentation of multiple individual α -Gal residues at the vesicle surface. Upon increasing the generation of the dendrons in **L-G1-Gal** and **L-G2-Gal**, thereby increasing the multivalency of the α -Gal to 2 and 4 per molecule respectively, the binding actually decreased. It is possible that the increase in multivalency was not sufficient to compensate for increasing steric hindrance that could prevent access of α -Gal on the vesicle surface to the binding site on the protein. The lectin-binding properties of libraries of carbohydrate-functionalized dendrimersomes expressing one or two carbohydrates per molecule have been previously reported.^{31, 33, 34} Using a hemagglutination assay, it was found that the carbohydrate affinity to the lectin was highly dependent on the architecture of the dendrimer. Highest binding (per carbohydrate) was observed when the carbohydrate was sterically unencumbered, although binding was higher when a two carbohydrates per molecule were present.

Upon further increasing the multivalency and changing from a vesicular to micellar morphology in **L-G3-Gal** and **L-G4-Gal**, the binding affinity increased significantly. Improved binding of small carbohydrate-functionalized micelles in comparison with analogous larger vesicles has been previously reported and was proposed to result from their higher curvature, though the reasons for this were not fully understood.⁸¹ It is possible that the packing requirements associated with the formation of the vesicle membrane inhibit mobility of the

carbohydrates and thus their binding abilities. The improved binding of the micellar structures relative to the vesicles might also be attributed to the lack of crystallinity of these systems (Table 1), which would also afford increased flexibility and adaptability of the system. The exchange of amphiphiles between polymeric micelles is well established and has been studied by techniques such as fluorescence spectroscopy.^{82, 83} However, the increased multivalency afforded by the G4 system is also clearly important as evidenced by the better binding of **L-G4-Gal**. This would result in increasingly high, localized concentrations of α -Gal, which can enhance binding through a proximity effect that may be more pronounced than a proximity effect over the assembly surface. A crystal structure of a GSL 1 isolectin has revealed that this lectin is tetrameric with a single carbohydrate binding site per subunit.⁸⁴ Basic molecular modeling has suggested that the α -Gal moieties on the G4 dendron can span a distance of ~ 3.5 nm, so it is unlikely that a single dendron can span multiple binding sites on the protein.³⁸

After the second washing procedure, the fluorescence of the **L-G0-Gal** system was nearly undetectable and became lower than **L-G1-Gal** and **L-G2-Gal**, which were poorer binders after the first wash. As the **L-G0-Gal** system exhibits the highest CAC value, more than 2-fold higher than the corresponding G1 system, it would be more likely to undergo disassembly and consequent loss of multivalency during the dilutions associated with the washing procedure, which took place over 3 hours. To probe this further, the disassembly kinetics of **L-G0-Gal** was probed by DLS. Assemblies were prepared above the CAC (0.5 mg/mL), then diluted to below the CAC (0.075 mg/mL). Following dilution, a gradual decrease in the count rate was observed, reaching $\sim 57\%$ of the initial value after 20 hours (Figure S90). The count rate was still ~ 100 -fold higher than that measured for buffer alone, suggesting that some assemblies were still present at this time. The time scale of the disassembly suggests that assemblies of **L-G0-Gal** were likely

not destroyed during dilutions associated with the first wash, but may have started to become disassociated during the second washing procedure, thereby compromising their ability to bind to the beads.

Only **L-G4-Gal** retained strong binding, with a normalized bead fluorescence ~6-fold higher than the next best system, **L-G3-Gal**. This can be attributed to this system exhibiting the highest multivalency and also the highest thermodynamic stability, as evidenced by its CAC. Thus, despite the complex interplay of different factors including molecular-level multivalency, assembly morphology, and assembly stability, it appears that assemblies formed from higher generation dendron-lipid hybrids are able to provide enhanced binding to the lectin-coated agarose beads. This can be attributed to their high multivalency, micellar morphology and high thermodynamic stability. Based on the results of the G0 through G2 systems, it is possible that thinning the carbohydrate density might lead to further improvements in binding.

Biological evaluation

The dendron-lipid hybrids were also investigated for their biological activity, specifically their ability to elicit a response from CD1d-restricted *i*NKT cells. CD1d is structurally similar to MHC class I molecules. However, unlike highly diverse MHC I molecules that present a wide range of peptide antigens to conventional T cells, the monomorphic CD1d presents select lipids to *i*NKT cells, infrequent but potent unconventional T cells with profound immunoregulatory roles in health and disease.^{85, 86} The prototypic CD1d-restricted agonist of *i*NKT cells is KRN 7000 that has an α -galactosylceramide structure.⁸⁷ The canonical T cell receptor (TCR) of *i*NKT cells interacts with both CD1d and the glycolipid it presents, which is typically followed by cytokine production.⁸⁸ It is noteworthy that the TCR of *i*NKT cells can also be triggered by

superantigens, exotoxins secreted by staphylococci and streptococci, in a CD1d-independent fashion.⁸⁹

The glycodendrons generated in this study are significantly different from natural CD1d ligand. However, the high concentration of α -Gal on the surfaces of the assemblies is reminiscent of the high carbohydrate content of the glycolipid-containing cell walls of certain bacterial species that are known to activate *i*NKT cells directly.^{90, 91} Two different sample preparation methods were investigated: 1) The assemblies prepared at 1 mg/mL, well above the CAC of all compounds, and then diluted to either 1 μ g/mL or 20 ng/mL for the bioassay we employed; 2) Compounds directly dissolved at 10 μ g/mL, which is approximately equal to or below the CAC for all compounds, and then diluted to either 1 μ g/mL or 20 ng/mL for the assay. Mouse DN32.D3 cells, a routinely used mouse *i*NKT hybridoma,⁹² were selected for the study. The co-expression of CD1d and the canonical TCR of *i*NKT cells by DN32.D3 cells allows these cells to cross-activate each other once exposed to antigenic glycolipids. This eliminates the need for the presence of accessory antigen-presenting cells in the assay, which could otherwise complicate the interpretation of the data. Cells were incubated with the indicated compounds or with 100 ng/mL of KRN 7000 (positive control) for 24 hours before the interleukin-2 (IL-2) content of culture supernatants was determined, as a measure of cellular activation, by a standard enzyme-linked immunosorbent assay (ELISA).⁸⁹

As shown in Figure 5, all dendron-lipid hybrids exhibited lower activity than KRN 7000. However, **L-G2-Gal**, **L-G3-Gal**, and **L-G4-Gal** exhibited higher activity than media alone or **L-G3-OH**. This is significant due to the substantial structural differences between the dendron-lipid hybrids and the natural ligands for the CD1d receptor. Previous work has shown that even small changes in the structure of α -galactosyl ceramides can result in complete loss of the

immunostimulatory response.⁹³ Interestingly, there was a trend towards higher activity for the samples that were prepared via direct dissolution at 10 $\mu\text{g/mL}$. This suggests that it was individual molecules rather than the assemblies that were interacting with the targets. It is possible that the preparation of samples at lower concentration prevents the irreversible formation of larger aggregates, such that those observed for **L-G3-Gal** and **L-G4-Gal**, which could prevent access to the α -Gal moieties. Nevertheless, in the *in vivo* application of these systems, self-assembly may still be expected to play a key role in dictating the biodistribution behavior of the materials, assuming that they would be administered at a dose above the CAC. The activity was also similar at concentrations of 20 ng/mL or 1 $\mu\text{g/mL}$, suggesting saturation of the receptor. Despite this, in each series of data there was a clear trend toward higher activity for the higher generation systems. This suggests that carbohydrate binding played a key role in the relevant ligand-receptor interactions and that the higher multivalency and/or size of the higher generation systems resulted in increased cellular activation. Further research will be required to elucidate the mechanism of action of these molecules and to explore their potential applications.

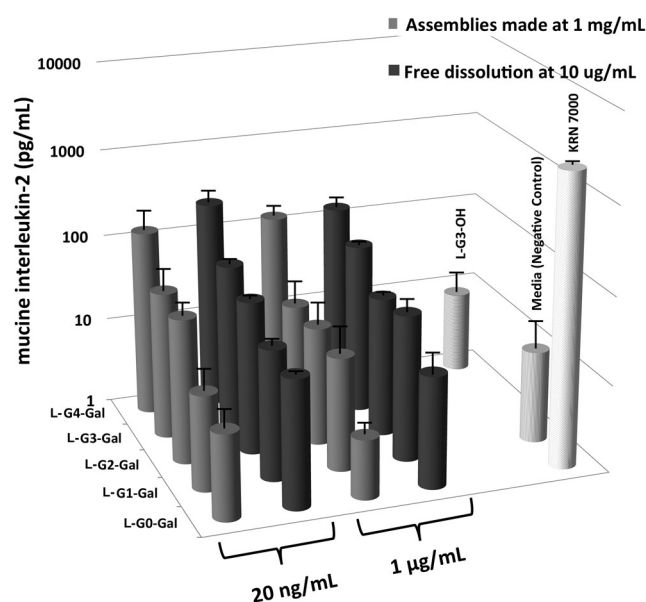


Figure 5. Levels of murine IL-2 following exposure to α -Gal-dendron-lipid hybrids, prepared as diluted assemblies or via direct dissolution and dilution, at either 20 ng/mL or 1 μ g/mL. The right column includes KRN 7000 at 100 ng/mL as a positive control, as well as **L-G3-OH** at 1 μ g/mL and media alone as negative controls. Error bars represent the standard deviation of 3 measurements.

Conclusions

The synthesis and study of the first glycodendron-lipid hybrids based on glycerides were described. A modular synthetic approach afforded hybrids containing two stearate chains and five different generations of dendrons functionalized on their peripheries with 1 to 16 C-linked α -Gal moieties. These materials self-assembled in aqueous solution through a solvent exchange method to form vesicles at low dendron generations and micelles at higher dendron generations. The CACs were in the nM range and decreased with increasing generation. This was attributed to the increasing molar mass of the amphiphiles with increasing generation, despite the corresponding increase in hydrophilic mass fraction, which would otherwise be expected to increase the CAC. The binding to GSL 1-coated agarose beads was studied using fluorescent dye-loaded assemblies. While GSL 1 is known to be specific for α -Gal residues, the current study confirmed for the first time the interaction between this lectin and a C-linked α -Gal. The study also revealed that assemblies prepared from higher dendron generations exhibited enhanced binding to GSL 1, a result that was attributed to a combination of factors arising from the increased adaptabilities of these systems, their higher multivalency, and their increased stability. Finally, the ability of the new dendron-lipid hybrids to activate *i*NKT cells was demonstrated, with enhanced activation observed for the higher generation systems. This effect

has not been previously noted for glycodendrons in any form, or for molecules with such significant structural differences from native α -galactosylceramides. Overall, the successful synthesis as well as the physical and biological evaluation of these materials demonstrates that glycodendron-lipid hybrids and their self-assemblies exhibit tunable properties and show promise for a variety of applications requiring specific receptor-ligand interactions.

Acknowledgements

Support received through the Canada Research Chairs program, the Natural Sciences and Engineering Research Council of Canada and the Canadian Institutes of Health Research is acknowledged. The authors thank Karen Nygard from the Western University Biotron for assistance with the fluorescence imaging.

Electronic supporting information

Full experimental procedures, ^1H and ^{13}C NMR spectra for all new compounds. DSC, DLS, CAC, and fluorescence data.

References

1. A. Fernández-Tejada, F. J. Cañada and J. Jiménez-Barbero, *Chem. - Eur. J.*, 2015, **21**, 10616-10628.
2. K. M. Fulton, *Curr. Top. Biochem. Res.*, 2012, **14**, 39-71.
3. E. Maverakis, K. Kim, M. Shimoda, M. E. Gershwin, F. Patel, R. Wilken, S. Raychaudhuri, L. R. Ruhaak and C. B. Lebrilla, *J. Autoimmun.*, 2015, **57**, 1-13.
4. S. S. Pinho and C. A. Reis, *Nat. Rev. Cancer*, 2015, **15**, 540-555.

5. S. V. Glavey, D. Huynh, M. R. Reagan, S. Manier, M. Moschetta, Y. Kawano, A. M. Roccaro, I. M. Ghobrial, L. Joshi and M. E. O'Dwyer, *Blood Rev.*, 2015, **29**, 269-279.
6. H. Lis and N. Sharon, *Chem. Rev.*, 1998, **98**, 637-674.
7. Y. Suzuki, T. Ito, T. Suzuki, R. E. Holland, T. M. Chambers, M. Kiso, H. Ishida and Y. Kawaoka, *J. Virol.*, 2000, **74**, 11825-11831.
8. J.-H. Kim, R. Resende, T. Wennekes, H.-M. Chen, N. Bance, S. Buchini, A. G. Watts, P. Pilling, V. A. Streltsov, M. Petric, R. Liggins, S. Barrett, J. L. McKimm-Breschkin, M. Niikura and S. G. Withers, *Science*, 2013, **340**, 71-75.
9. J. Singh, R. C. Petter, T. A. Baillie and A. Whitty, *Nat. Rev. Drug Discov.*, 2011, **10**, 307-317.
10. T. K. Lindhorst and M. Dubber, *Carbohydr. Res.*, 2015, **403**, 90-97.
11. R. J. Pieters, *Org. Biomol. Chem.*, 2009, **7**, 2013-2025.
12. J. L. Jimenez Blanco, C. Ortiz Mellet and J. M. Garcia Fernandez, *Chem. Soc. Rev.*, 2013, **42**, 4518-4531.
13. N. Kottari, Y. M. Chabre, R. Sharma and R. Roy, in *Multifaceted Development and Application of Biopolymers for Biology, Biomedicine and Nanotechnology*, eds. P. K. Dutta and J. Dutta, Springer, Berlin, Heidelberg, 2013, vol. 254, pp. 297-341.
14. M. A. van Dongen, C. A. Dougherty and M. M. Banaszak Holl, *Biomacromolecules*, 2014, **15**, 3215-3234.
15. K. Lin and A. M. Kasko, *Bioconjugate Chem.*, 2015, **26**, 1504-1512.
16. A. K. Adak, B.-Y. Li and C.-C. Lin, *Carbohydr. Res.*, 2015, **405**, 2-12.
17. K. Sun, S. W. A. Bligh, H.-L. Nie, J. Quan and L.-M. Zhu, *RSC Adv.*, 2014, **4**, 34912-34921.

18. C. Bonduelle, J. Huang, T. Mena-Barragán, C. Ortiz Mellet, C. Decroocq, E. Etamé, A. Heise, P. Compain and S. Lecommandoux, *Chem. Commun.*, 2014, **50**, 3350-3352.
19. T. Imura, N. Ohta, K. Inoue, N. Yagi, H. Negishi, H. Yanagishita and D. Kitamoto, *Chem. - Eur. J.*, 2006, **12**, 2434-2440.
20. D. Kitamoto, T. Morita, T. Fukuoka, M.-a. Konishi and T. Imura, *Curr. Opin. Colloid Interface Sci.*, 2009, **14**, 315-328.
21. S. Egli, H. Schlaad, N. Bruns and W. Meier, *Polymers*, 2011, **3**, 252.
22. J. Huang, C. Bonduelle, J. Thévenot, S. Lecommandoux and A. Heise, *J. Am. Chem. Soc.*, 2011, **134**, 119-122.
23. J. R. Kramer, A. R. Rodriguez, U.-J. Choe, D. T. Kamei and T. J. Deming, *Soft Matter*, 2013, **9**, 3389-3395.
24. G. Whitton and E. R. Gillies, *J. Polym. Sci. A: Polym. Chem.*, 2015, **53**, 148-172.
25. I. Gitsov, *Encyclopedia of Polymeric Nanomaterials*, 2015, 2436-2446.
26. S. Garcia Gallego, A. Nyström and M. Malkoch, *Prog. Polym. Sci.*, 2015, **48**, 85-110.
27. C. M. Dong and G. Liu, *Polym. Chem.*, 2013, **4**, 46-52.
28. A. L. Martin, B. Li and E. R. Gillies, *J. Am. Chem. Soc.*, 2009, **131**, 734-741.
29. A. Nazemi, S. M. M. Haeryfar and E. R. Gillies, *Langmuir*, 2013, **29**, 6420-6428.
30. M. Dubber, A. Patel, K. Sadalpure, I. Aumüller and T. K. Lindhorst, *Eur. J. Org. Chem.*, 2006, **2006**, 5357-5366.
31. S. Zhang, R.-O. Moussodia, H.-J. Sun, P. Leowanawat, A. Muncan, C. D. Nusbaum, K. M. Chelling, P. A. Heiney, M. L. Klein, S. André, R. Roy, H.-J. Gabius and V. Percec, *Angew. Chem. Intl. Ed.*, 2014, **53**, 10899-10903.

32. S. Zhang, Q. Xiao, S. E. Sherman, A. Muncan, A. D. M. Ramos Vicente, Z. Wang, D. A. Hammer, D. Williams, Y. Chen, D. J. Pochan, S. Vértesy, S. André, M. L. Klein, H.-J. Gabius and V. Percec, *J. Am. Chem. Soc.*, 2015, **137**, 13334-13344.
33. S. Zhang, R.-O. Moussodia, C. Murzeau, H.-J. Sun, M. L. Klein, S. Vértesy, S. André, R. Roy, H.-J. Gabius and V. Percec, *Angew. Chem. Intl. Ed.*, 2015, **54**, 4036-4040.
34. V. Percec, P. Leowanawat, H.-J. Sun, O. Kulikov, C. D. Nusbaum, T. M. Tran, A. Bertin, D. A. Wilson, M. Peterca, S. Zhang, N. P. Kamat, K. Vargo, D. Moock, E. D. Johnston, D. A. Hammer, D. J. Pochan, Y. Chen, Y. M. Chabre, T. C. Shiao, M. Bergeron-Brlek, S. André, R. Roy, H.-J. Gabius and P. A. Heiney, *J. Am. Chem. Soc.*, 2013, **135**, 9055-9077.
35. Q. Xiao, S. Zhang, Z. Wang, S. E. Sherman, R.-O. Moussodia, M. Peterca, A. Muncan, D. R. Williams, D. A. Hammer, S. Vértesy, S. André, H.-J. Gabius, M. L. Klein and V. Percec, *Proc. Natl. Acad. Sci. U. S. A.*, 2016, **113**, 1162-1167.
36. T. Takahashi, E. Yuba, C. Kojima, A. Harada and K. Kono, *Res. Chem. Int.*, 2009, **35**, 1005-1014.
37. K. Torigoe, A. Tasaki, T. Yoshimura, K. Sakai, K. Esumi, Y. Takamatsu, S. C. Sharma, H. Sakai and M. Abe, *Colloids Surf., A*, 2008, **326**, 184-190.
38. A. Peyret, J. F. Trant, C. V. Bonduelle, K. Ferji, N. Jain, S. Lecommandoux and E. R. Gillies, *Polym. Chem.*, 2015, **6**, 7902-7912.
39. G. Huang, F. Cheng, X. Chen, D. Peng, X. Hu and G. Liang, *Curr. Pharm. Design*, 2013, **19**, 2454-2458.
40. M. Marradi, F. Chiodo, I. García and S. Penadés, *Chem. Soc. Rev.*, 2013, **42**, 4728-4745.
41. G. Pasut, D. Paolino, C. Celia, A. Mero, A. S. Joseph, J. Wolfram, D. Cosco, O. Schiavon, H. Shen and M. Fresta, *J. Controlled Release*, 2015, **199**, 106-113.

42. P. Degen, D. C. F. Wieland and C. Strötges, *Langmuir*, 2015, **31**, 11851-11857.
43. P. Degen, M. Wyszogrodzka and C. Strötges, *Langmuir*, 2012, **28**, 12438-12442.
44. Y. Liu, Y. Ng, M. R. Toh and G. N. C. Chiu, *J. Controlled Release*, 2015, **220A**, 438-446.
45. S. J. van Vliet, E. Saeland and Y. van Kooyk, *Trends Immunol.*, 2008, **29**, 83-90.
46. U. Galili, *Immunol. Cell Biol.*, 2005, **83**, 674-686.
47. T. Natori, Y. Koezuka and T. Higa, *Tetrahedron Lett.*, 1993, **34**, 5591-5592.
48. T. Natori, M. Morita, K. Akimoto and Y. Koezuka, *Tetrahedron*, 1994, **50**, 2771-2784.
49. K. O. A. Yu and S. A. Porcelli, *Immunol. Lett.*, 2005, **100**, 42-55.
50. D. C. Koester, A. Holkenbrink and D. B. Werz, *Synthesis*, 2010, **19**, 3217-3242.
51. B. Vauzeilles, D. Urban, G. Doisneau and J.-M. Beau, in *Glycoscience*, ed. H. Kondo, Springer, New York, 2008, ch. 9.4, pp. 2021-2078.
52. G. Yang, J. Schmiege, M. Tsuji and R. W. Franck, *Angew. Chem. Intl. Ed.*, 2004, **43**, 3818-3822.
53. O. L. Padilla De Jesús, H. R. Ihre, L. Gagne, J. M. J. Fréchet and F. C. Szoka, *Bioconjugate Chem.*, 2002, **13**, 453-461.
54. E. R. Gillies, E. Dy, J. M. J. Fréchet and F. C. Szoka, *Mol. Pharmaceutics*, 2005, **2**, 129-138.
55. P. Wu, M. Malkoch, J. N. Hunt, R. Vestberg, E. Kaltgrad, M. G. Finn, V. V. Fokin, K. B. Sharpless and C. J. Hawker, *Chem. Commun.*, 2005, 5775-5777.
56. S. García-Gallego, D. Hult, J. V. Olsson and M. Malkoch, *Angew. Chem. Intl. Ed.*, 2015, **54**, 2416-2419.
57. B. Li, A. L. Martin and E. R. Gillies, *Chem. Commun.*, 2007, 5217-5219.

58. N. Feliu, M. V. Walter, M. I. Montañez, A. Kunzmann, A. Hult, A. Nyström, M. Malkoch and B. Fadeel, *Biomaterials*, 2012, **33**, 1970-1981.
59. S. Mourtas, M. Canovi, C. Zona, D. Aurilia, A. Niarakis, B. La Ferla, M. Salmona, F. Nicotra, M. Gobbi and S. G. Antimisiaris, *Biomaterials*, 2011, **32**, 1635-1645.
60. V. V. Rostovtsev, L. G. Green, V. V. Fokin and K. B. Sharpless, *Angew. Chem. Intl. Ed.*, 2002, **41**, 2596-2599.
61. C. J. Capicciotti, J. F. Trant, M. Leclère and R. N. Ben, *Bioconjugate Chem.*, 2011, **22**, 605-616.
62. S. Zhang, H.-J. Sun, A. D. Hughes, R.-O. Moussodia, A. Bertin, Y. Chen, D. J. Pochan, P. A. Heiney, M. L. Klein and V. Percec, *Proc. Natl. Acad. Sci. U. S. A.*, 2014, **111**, 9058-9063.
63. K. Kalyanasundaram and J. K. Thomas, *J. Am. Chem. Soc.*, 1977, **99**, 2039-2044.
64. G. Basu Ray, I. Chakraborty and S. P. Moulik, *J. Colloid Interface Sci.*, 2006, **294**, 248-254.
65. F. R. Hallett, J. Watton and P. Krygsman, *Biophys. J.*, 1991, **59**, 357-362.
66. N. W. Suek and M. H. Lamm, *Langmuir*, 2008, **24**, 3030-3036.
67. P. M. Nguyen and P. T. Hammond, *Langmuir*, 2006, **22**, 7825-7832.
68. V. Istratov, H. Kautz, Y. K. Kim, R. Schubert and H. Frey, *Tetrahedron*, 2003, **59**, 4017-4024.
69. I. Lynch, J. Sjöström and L. Piculell, *J. Phys. Chem. B*, 2005, **109**, 4252-4257.
70. I. Goldstein and H. Winter, in *α -Gal and Anti-Gal*, eds. U. Galili and J. Avila, Springer US, 1999, vol. 32, ch. 6, pp. 127-141.
71. R. Kaifu, L. C. Plantefaber and I. J. Goldstein, *Carbohydr. Res.*, 1985, **140**, 37-49.

72. L. A. Murphy and I. J. Goldstein, *Biochemistry*, 1979, **18**, 4999-5005.
73. N. Sharon, *J. Biol. Chem.*, 2007, **282**, 2753-2764.
74. Y. Takeda and I. Matsuo, in *Lectins: Methods and Protocols*, ed. J. Hirabayashi, Humana Press, New York, 2014, ch. 18, pp. 207-214.
75. K. Sano and H. Ogawa, in *Lectins: Methods and Protocols*, ed. J. Hirabayashi, Humana Press, New York, 2014, ch. 4, pp. 47-52.
76. W. Wang, D. Chance, V. Mossine and T. Mawhinney, *Glycoconjugate J.*, 2014, **31**, 133-143.
77. P. Greenspan, E. P. Mayer and S. D. Fowler, *J. Cell Biol.*, 1985, **100**, 965-973.
78. Z. Pang, N. E. Laplante and R. J. Filkins, *J. Microsc.*, 2012, **246**, 1-10.
79. B. Chatterjee, P. Vaith, S. Chatterjee, D. Karduck and G. Uhlenbruck, *Int. J. Biochem.*, 1979, **10**, 321-327.
80. A. M. Wu, J. H. Wu, L.-H. Lin, S.-H. Lin and J.-H. Liu, *Life Sci.*, 2003, **72**, 2285-2302.
81. B. S. Kim, D. J. Hong, J. Bae and M. Lee, *J. Am. Chem. Soc.*, 2005, **127**, 16333-16337.
82. K. Procháazka, B. Bednár, E. Mukhtar, P. Svoboda, J. Trená and M. Almgren, *J. Phys. Chem.*, 1991, **95**, 4563-4568.
83. S. Creutz, J. van Stam, S. Antoun, F. C. De Schryver and R. Jérôme, *Macromolecules*, 1997, **30**, 4078-4083.
84. J. Lescar, R. Loris, E. Mitchell, C. Gautier, V. Chazalet, V. Cox, L. Wyns, S. Pérez, C. Breton and A. Imberty, *J. Biol. Chem.*, 2002, **277**, 6608-6614.
85. A. Bendelac, P. B. Savage and L. Teyton, *Annu. Rev. Immunol.*, 2007, **25**, 297-336.
86. M. J. van den Heuvel, N. Garg, L. Van Kaer and S. M. Haeryfar, *Trends Mol. Med.*, 2011, **17**, 65-77.

87. M. Morita, K. Motoki, K. Akimoto, T. Natori, T. Sakai, E. Sawa, K. Yamaji, Y. Koezuka, E. Kobayashi and H. Fukushima, *J. Med. Chem.*, 1995, **38**, 2176-2187.
88. N. A. Borg, K. S. Wun, L. Kjer-Nielsen, M. C. Wilce, D. G. Pellicci, R. Koh, G. S. Besra, M. Bharadwaj, D. I. Godfrey, J. McCluskey and J. Rossjohn, *Nature*, 2007, **448**, 44-49.
89. J. L. Hayworth, D. M. Mazzuca, S. M. Vareki, I. Welch, J. K. McCormick and S. M. M. Haeryfar, *Immunol. Cell Biol.*, 2012, **90**, 699-709.
90. Y. Kinjo, D. Wu, G. Kim, G.-W. Xing, M. A. Poles, D. D. Ho, M. Tsuji, K. Kawahara, C.-H. Wong and M. Kronenberg, *Nature*, 2005, **434**, 520-525.
91. Y. Kinjo, P. Illarionov, J. L. Vela, B. Pei, E. Girardi, X. Li, Y. Li, M. Imamura, Y. Kaneko, A. Okawara, Y. Miyazaki, A. Gomez-Velasco, P. Rogers, S. Dahesh, S. Uchiyama, A. Khurana, K. Kawahara, H. Yesilkaya, P. W. Andrew, C.-H. Wong, K. Kawakami, V. Nizet, G. S. Besra, M. Tsuji, D. M. Zajonc and M. Kronenberg, *Nat. Immunol.*, 2011, **12**, 966-974.
92. O. Lantz and A. Bendelac, *J. Exp. Med.*, 1994, **180**, 1097-1106.
93. A. Banchet-Cadeddu, E. Henon, M. Dauchez, J.-H. Renault, F. Monneaux and A. Haudrechy, *Org. Biomol. Chem.*, 2011, **9**, 3080-3104.